CAUSES OF CRACK FORMATION IN THE HAZ OF CAST HIGH-MANGANESE STEEL IN FLASH-BUTT WELDING

S.I. KUCHUK-YATSENKO, V.I. SHVETS, Yu.V. SHVETS, T.G. TARANOVA and **G.N. GORDAN**
E.O. Paton Electric Welding Institute, NASU, Kiev, Ukraine

Results of investigations of the causes of cracks forming in the HAZ of cast high-manganese steel 110G13L in its flash-butt welding to austenitic steel 08Kh18N10T are presented. It is shown that cracking is caused by segregational heterogeneity of distribution of phosphorus, which occurs both in solidification of castings and in the solid solution under thermal deformation conditions of welding. To prevent cracking, it is recommended to pay special attention to the process of homogenizing annealing of 110G13L castings.

Keywords: *flash-butt welding, pulsed flashing, high-manganese steel 110G13L, austenitic insert, frog, HAZ, phosphorus segregation, cracks*

Frogs are one of the most critical elements of railway tracks. Welded structures are widely used in their manufacture in the world. PWI developed technology and equipment for welding railway frogs in the shop [1]. This technology is based on the process of pulsed flash-butt welding [2], when a core of high-manganese 110G13L steel is joined to rail steel M76 through an intermediate insert from chromium-nickel austenitic steel 08Kh18N10T.

Outgoing inspection of some batches of welded frogs in a number of cases revealed cracks in the toe section in the near-weld zone of 110G13L steel after final machining (Figure 1), which were the cause for rejection of the finished product.

The objective of this work is establishing the causes for crack initiation in 110G13L steel and development of measures to prevent them.

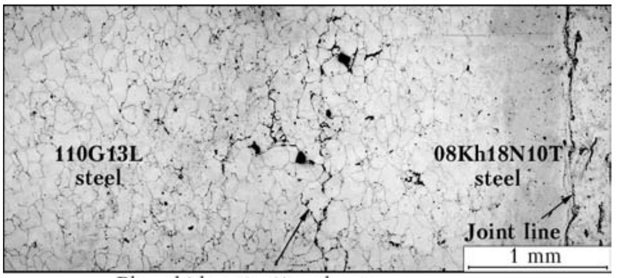

Figure 1. Macrostructure of fusion zone of 110G13L steel with 08Kh18N10T steel in the frog welded joint

Flash-butt welding was performed in K924M welding machine, developed at PWI, in the mode accepted for industrial production. Welding process duration was 90–110 s, welding allowance was (3.0 + 1.5) mm, insert width in the welded joint was 18–20 mm.

Analysis of microstructure and chemical heterogeneity of the HAZ of 110G13L steel joint was performed to reveal the causes for cracking. The cracked area and adjacent area without cracks were analyzed. Investigations were conducted in optical microscope «Neophot-32», microscope-microanalyser SX-50 of Camebax, scanning electron microscope JSM-840 with «Link-systems» microanalyser. Microstructure was revealed by electrolytic etching in 10 % water solution of ammonium triosulphate.

Spectral analysis of chemical composition of 110G13L steel, used in frog manufacture, corresponded to GOST 2176–77 (Table 1). Phosphorus and sulphur content was much lower than the standard requirement.

Macrostructure analysis showed (see Figure 1) that metal fracture in all the cases runs in a layer about 0.5 mm wide, which is located in parallel to the joint line at about 1.5–2.0 mm distance. Cracking is of intergranular nature, i.e. is concentrated on the boundaries of austenitic grains of 110G13L steel.

Investigations showed that metal of 110G13L steel joint has a stable austenitic structure with unit carbide inclusions and a considerable quantity of nonmetallic inclusions. Under the impact of thermal cycle of welding first a refinement of austenite grains occurs in the HAZ metal, and in the near-contact layer austenite grain size increases as a result of collective recrystallization. An austenitic structure with strength prop-

Table 1. Composition of 110G13L steel (wt.%)

Source	C	Mn	Si	S	P	Cr	Ni	Cu
GOST 2176–77	0.9–1.4	11.5–15.0	0.3–1.0	≤0.05	≤0.12	≤3.8	≤0.7	≤0.3
X-ray microprobe analysis	0.92–0.95	12.3–12.7	0.46	0.021–0.023	0.033–0.036	N/D	N/D	N/D

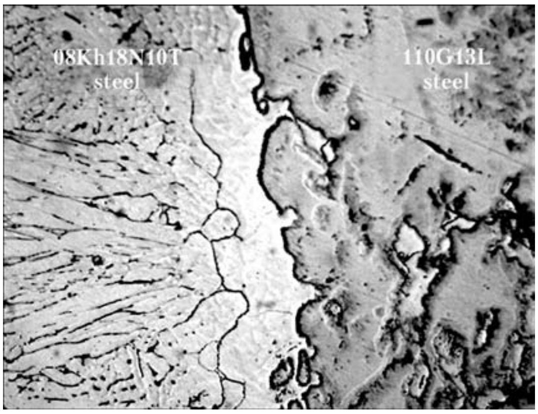

Figure 2. Microstructure (×400) of the transition zone on the contact line of fusion of 110G13L steel with 08Kh18N10T steel

erties on the level of those of base metal forms in the transition zone on the contact boundary of 110G13L steel with 08Kh18N10T steel (Figure 2). In the HAZ region at approximately 1.5–2.0 mm distance from the joint line, a certain structural component is present along the grain boundaries, which, obviously, is what causes the cracking. In areas with a high content of this structure an acicular phase forms from the grain boundaries (Figure 3).

Analysis of nonmetallic inclusions of 110G13L steel was performed to clarify the nature of formation of this structural component. It is established that the steel contains a considerable volume fraction of complex sulphides (Figure 4, *a, b*), the central part of which is made of aluminium sulphide, and the peripheral part are manganese and iron sulphides. There are also individual inclusions of aluminium sulphide. Clusters of fine nitride inclusions of a regular geometrical shape, as well as, possibly, titanium carbonitrides, non-uniformly distributed in the bulk, are also observed (Figure 4, *c*). Phosphide inclusions are absent. This is in agreement with the results of earlier investigations, which showed that phosphides could not be found even at 0.1 wt.% P in 110G13L steel [3].

Analysis of transformation of nonmetallic inclusions in the HAS showed that high-temperature nitrides remain stable up to steel melting temperature. Sulphide inclusions change only slightly compared to those in the base metal, at least in the section of the layer with the newly formed structural component. Thus, contamination of 110G13L steel by nonmetallic inclusions is not a source of formation of the above component.

According to the curves of chemical element distribution (Figure 5), an increase of manganese and phosphorus content is found at transition through grain boundaries with the new structural component. At analysis of the composition of accessible for study microvolumes at the junction of three grains, it is established that phosphorus and manganese content is equal to 12.040 and 29.826 wt.%, respectively (Table 2, No.1). This gives rise to the conclusion that cracking is caused by the described in literature proc-

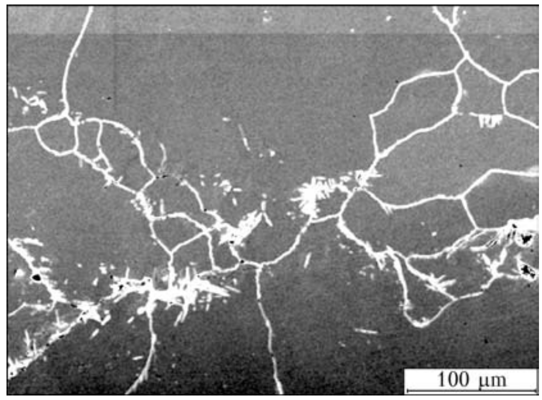

Figure 3. HAZ microstructure of 110G13L steel in the section with phosphide eutectics

ess of formation of a low-melting phosphide (carbophosphide at high carbon content) eutectic in manganese steels, embrittling the grain boundaries [4].

At 0.033–0.043 wt.% P content in 110G13L steel the cause for phosphide eutectic formation, evidently, is a local increase of this element concentration, caused by its non-uniform distribution. The latter can result,

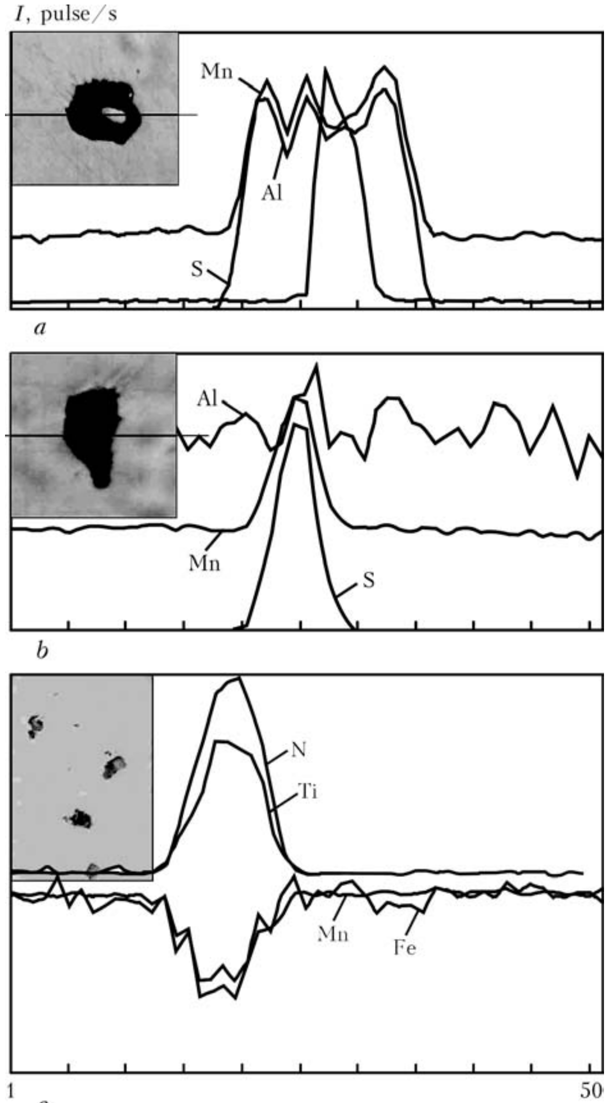

Figure 4. Distribution of chemical elements in sulphides (*a*, *b*) and nitrides (*c*) of 110G13L steel (*I* — radiation pulse; 1.02 μm step)

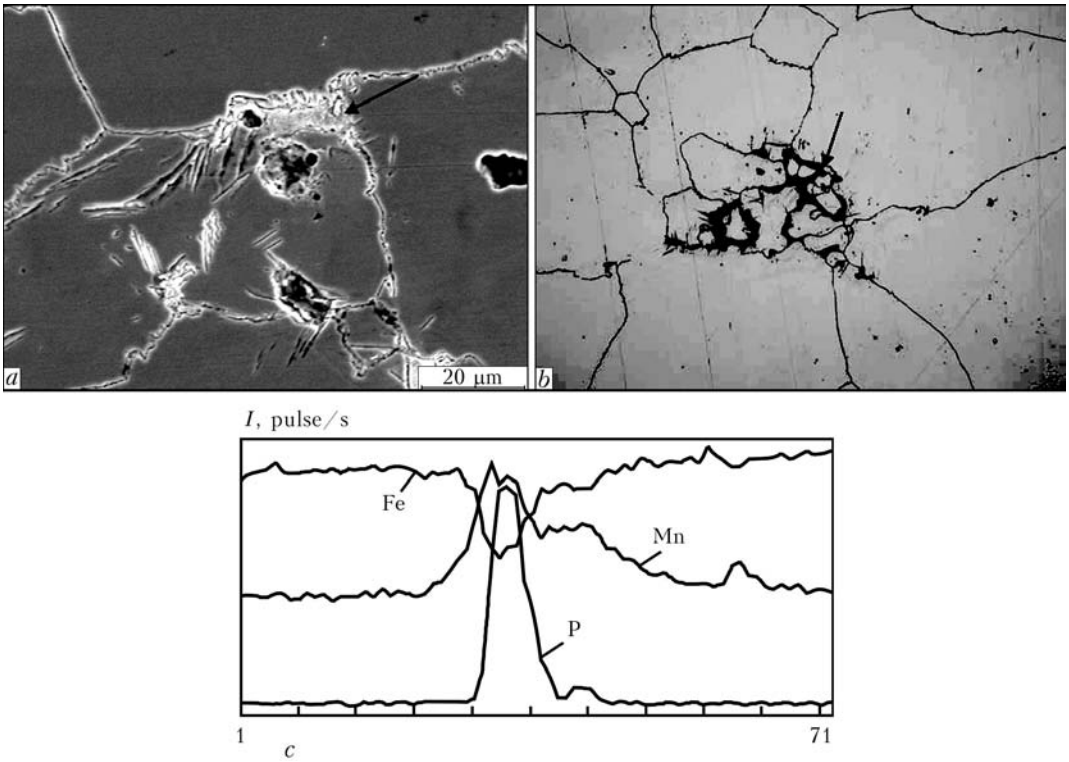

Figure 5. Carbophosphide eutectics in microstructure of 110G13L steel (marked by arrows): *a* — electron microscopy image; *b* — optical image (×400); *c* — distribution of chemical elements in the zone of carbophosphide eutectic (2 μm step)

primarily, from primary segregation — phosphorus greatly widens the temperature interval of steel solidification. Moreover, in welding segregation of surface-active phosphorus in the solid phase and grain boundary enrichment in it are possible in iron in the thermodeformational impact zone. This, obviously, occurs in the HAZ layer at 1.5–2.5 mm distance from the joint line, where the temperature is approximately equal to 900–1000 °C in welding.

It is known that the temperature of eutectic reaction $l \rightarrow \gamma\text{-Fe} + (Fe, Mn)_2P$ in Fe–Mn–P system is equal to about 950 °C [5]. Increase of phosphorus and manganese content on grain boundaries causes their concentration melting, which leads to development of the process of eutectic phase formation. Manganese, phosphorus, as well as carbon, actively diffuse into the melt, as their solubility in the liquid phase is by several orders of magnitude higher than in the solid phase.

Solidification of the formed intergranular melt occurs with formation of phosphide eutectics and acicular carbides growing from grain boundaries.

In the HAZ layer of 110G13L steel up to 1.5 mm wide adjacent to the joint line, the thermal impact corresponds to homogenizing annealing. Concentrational heterogeneity of phosphorus and manganese in this region is eliminated — intergranular eutectic interlayers are absent in the microstructure.

In the more remote HAZ regions diffusion mobility is insufficient to achieve phosphorus concentration on grain boundaries, at which partial melting occurs.

Thus, investigation results showed that in flash-butt welding conditions for formation of phosphide eutectics are in place in the HAZ metal of 110G13L steel at 1.5–2.0 mm distance from the joint line. As its formation occurs in an irregular manner, it is anticipated that the main cause for its appearance at average phosphorus content of 0.033–0.036 wt.% in steel is the non-uniformity of its distribution. Achievement of a uniform distribution of phosphorus in 110G13L steel is difficult because of its low diffusion mobility in iron. One of the ways to achieve a uniform distribution of phosphorus is to strictly follow the specified mode of homogenizing annealing of 110G13L

Table 2. Results of X-ray microprobe analysis of composition (wt.%) of the new structural component of the layer with microcracks in 110G13L steel

No	P	Si	Mn	Cr	Fe	C
1	12.040	0.434	29.826	0.438	52.182	5.054
2	2.234	0.659	21.361	0.213	73.352	2.181
3	1.298	0.634	18.148	0.163	78.561	1.195
4	3.534	0.672	21.936	0.214	71.428	2.204

steel castings; another one is to lower phosphorus content. In order to prevent cracks in manganese steels the recommended phosphorus content should be less than 0.02 wt.% [4, 5].

CONCLUSIONS

1. In manufacture of rail frogs by flash-butt welding low-melting intergranular interlayers of phosphide eutectics causing cracking, can form at the distance of 1.5–2.5 mm from the joint line in the HAZ metal of 110G13L steel.

2. Formation of intergranular interlayers of phosphide eutectics at phosphorus content of 0.033–0.036 wt.% is caused by segregational heterogeneity of its distribution at solidification of castings.

3. To prevent formation of intergranular interlayers of phosphide eutectics in the HAZ of 110G13L steel it is necessary to strictly follow the established mode of homogenizing annealing of castings from 110G13L steel.

1. *TU U DP 32-4520.13.500-007-2002:2006*: Crossing and frogs with welded rail ends of R65, R50 and USC60 type with and without insert. Test batch. Valid from 01.01.2003 to 01.01.2006.
2. Kuchuk-Yatsenko, S.I., Shvets, Yu.V., Dumchev, E.A. et al. (2005) Flash butt welding of railway frogs with rail ends using an intermediate insert. *The Paton Welding J.*, **1**, 2–4.
3. Ershov, G.S., Poznyak, L.A. (1998) *Formation of structure and properties of steels and alloys*. Kiev: Naukova Dumka.
4. Kondratyuk, S.E., Kasatkin, O.G. (1987) *Fracture of cast manganese steel*. Kiev: Naukova Dumka.
5. Goudremont, E. (1960) *Special steels*. Vol. 2. Moscow: Metallurgizdat.

PROBABILISTIC CHARACTERISTICS OF HIGH-CYCLE FATIGUE RESISTANCE OF STRUCTURAL STEEL WELDED JOINTS

V.I. MAKHNENKO and **I.Yu. ROMANOVA**
E.O. Paton Electric Welding Institute, NASU, Kiev, Ukraine

Issues of probabilistic determination of resistance of welded joints to high-cycle fatigue fracture are considered. The probability of failure-free performance of the joints for different types and variable values of applied loads is analysed.

Keywords: *welded joints, cyclic loading, high-cycle fatigue, fatigue resistance, probabilistic prediction methods, safe operation*

The growth of interest has been noted lately in probabilistic methods for estimation of beginning of the limiting state of welded joints under different loads, this being associated to a substantial degree with a large number of factors taking place within the joining zone and affecting the beginning of the limiting state. This is particularly important for alternating loads and fatigue fractures of welded joints. The presence of many factors, which are hard to describe in deterministic expressions, leads to a wide spread of data of fatigue tests of the welded joints.

The use of stochastic methods for calculation of fatigue of the welded joints requires clear ideas of the probabilistic characteristics of fatigue fracture resistance of welded joints on different structural materials. Such characteristics for certain welded joints and materials (mainly structural steels) in the form of a range of variations of normal rated stresses, $\Delta\sigma$, and probability of fracture were obtained experimentally [1–3, etc.].

The efforts of the International Institute of Welding (IIW) [4], dedicated to high-cycle fatigue of welded joints on ferritic-pearlitic structural steels with strength of up to 900 MPa showed that at failure probability $Q_p = 5\cdot10^{-2}$ (no-fracture probability is $9.5\cdot10^{-1}$) the fatigue fracture resistance can be sufficiently reliably described by rated stress ranges *FAT* on a base of $N = 2\cdot10^6$ cycles. In this case, the permissible ranges under regular cyclic loading are determined by the following relationship [4]:

$$[\Delta\sigma] = FAT\,\frac{f_1(N)f_2(R)}{\gamma_m f_3(\delta)}, \qquad (1)$$

where $f_1(N)$, $f_2(R)$ and $f_3(\delta)$ are the corrections for durability N, cycle asymmetry R and thickness δ of a workpiece welded (at $N < 2\cdot10^6$ cycles, $R \geq 0.5$ and $\delta > 25$ mm, each of these corrections is more than 1); γ_m is the safety factor equal to 1.0–1.4, i.e. at $f_1 = f_2 = f_3 = 1$ and $\gamma_m = 1$ the failure probability is guaranteed at a level of approximately 0.05.

Naturally, safety grows at $\gamma_m > 1$, and the failure probability dramatically decreases as a result of fatigue fracture.

Considering the IIW recommendations [4], it is of high practical interest to supplement them with the data on fracture probability for different *FAT* values and classes K_x of the joints, depending on the required value of durability N and load level $\Delta\sigma$. For this purpose it is possible to use the already published experimental results on fracture probability of different types of the welded joints, by relating these data to the recommendations given in [4]. The search for